ACS OMEGA

http://pubs.acs.org/journal/acsodf

Article

Long-Wavelength Absorbing Benzimidazolo-Chlorin for Enhanced Photodynamic Therapy

Huiqiang Wu, Sooho Yeo, Jiazhu Li,* Jinjun Wang, Woo Kyoung Lee,* and Il Yoon*

Cite This: *ACS Omega* 2023, 8, 21941−21947

Read Online

ACCESS | Metrics & More | Article Recommendations | Supporting Information

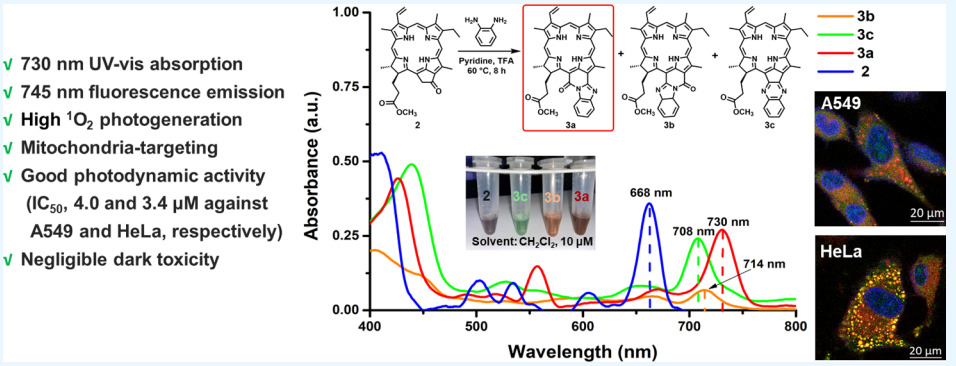

ABSTRACT: In this study, we condensed methyl pyropheophorbide-a (**2**) with 1,2-phenylenediamine to synthesize benzimidazolo-chlorin (**3a**) as an effective near-infrared photosensitizer (PS) with an absorption maximum of 730 nm. The ability of **3a** to generate singlet oxygen, as well as its photodynamic effect on A549 and HeLa cells, was investigated. PS exhibited strong phototoxicity and negligible dark toxicity. Its structure was examined by UV−visible spectroscopy, nuclear magnetic resonance, and high-resolution fast atom bombardment mass spectrometry.

INTRODUCTION

Photodynamic therapy (PDT), a noninvasive and patient-friendly cancer treatment, has gained popularity in recent decades.[1,2] PDT is now an extremely common treatment modality because of its high responsiveness and tumor-localizing treatment,[3] which reduces long-term morbidity and sets PDT apart from many other cancer treatments, such as chemotherapy, radiotherapy, and tumor resection.

In general, irradiating the tumor site with a suitable wavelength[4] can activate photosensitizers (PSs) that have selectively accumulated in the tumor tissue, causing a photochemical reaction, which results in the necrosis of the tumor tissue.[5−7] It can only be applied to shallow tissues due to low penetration and the absorption of surrounding tissues.[8] As a result, a key parameter of ideal PS is the absorption ability of light in the long-wavelength region, where sufficient tissue penetration by PS-activating light, known as the therapeutic window,[9−12] can be achieved for overcoming the aforementioned shortcomings, resulting in deeper tumor treatment without side effects.

PSs can be modified via either chemical conjugation or physical coupling, which manipulates their chemical properties, such as absorbance, solubility, singlet oxygen ($^1O_2$), photogeneration quantum yield, and tissue penetration. Chlorin derivatives are chemically and thermally stable long-wavelength absorbing PSs with strong Soret and Q band absorption. For synthesizing these, it is important to use chlorophyll-a with various chemical modifications, such as a fused cyclopentanone structure (E ring), for increased long-wavelength absorption of PS, as shown in Scheme 1.[13−18]

Benzimidazole, a key component of vitamin B12, is a benzoheterocyclic compound containing two nitrogen atoms. There have been numerous reports of benzimidazole derivatives with anticancer activity.[19−21] Furthermore, benzimidazole is an effective chromophore that combines with chlorophyll-a and conjugates with porphyrin rings, increasing electron delocalization and causing a red-shift of the maximum absorption wavelength to synthesize long-wavelength absorbing PS.[22,23]

Pandey et al. recently reported benzimidazole-introduced chlorin derivatives by synthesizing methyl 13^2-oxopyropheophorbide-a (13^2-oxo-methyl pyropheophorbide a (MPPa)) via LiOH-promoted allomerization of PPa, followed by con-

Received: March 17, 2023
Accepted: May 25, 2023
Published: June 6, 2023

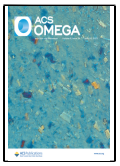

Scheme 1. Synthetic Procedure of Benzimidazolo-Chlorin Isomers (3a and 3b) and Fused Quinoxaline (3c)[a]

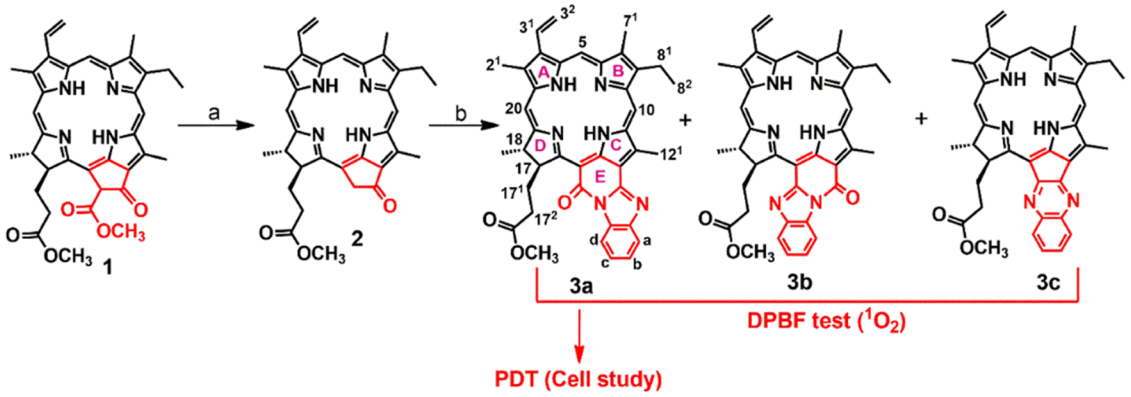

[a]$^1O_2$ Photogeneration ability of compounds **3a**, **3b**, and **3c** was evaluated by 1,3-diphenylisobenzofuran (DPBF) test, from which **3a** was used for cell study (PDT activity). (a) Pyridine, H_2O, N_2, reflux, 8 h, 80%; (b) 1,2-Phenylenediamine, pyridine, trifluoroacetic acid, N_2, reflux, 8 h, diazomethane (**3a**: 20%, **3b**: 10%, **3c**: 2.5%).

densation of 13^2-oxo-MPPa with 1,2-phenylenediamine with an acid catalyst (two-step synthetic procedure).[24]

Furthermore, Pandey et al. synthesized benzimidazolo-bacterochlorin derivatives, which displayed red-shifted long-wavelength absorption in the near-infrared (NIR) region and were highly stable as potential PS candidates for PDT.[25] In a previous study, we synthesized benzimidazolo-chlorin isomers **3a** and **3b** and fused them with quinoxaline **3c** from methyl pheophorbide-a (MPa, **1**) or MPPa (**2**) after a condensation reaction with 1,2-phenylenediamine.[26]

To the best of our knowledge, this is the first cell study on PDT using compound **3a**. As a result, in this study, we revisited the synthesis of chlorin derivatives **3a**, **3b**, and **3c** to develop a long-wavelength absorbing promising PS for enhanced PDT.

RESULTS AND DISCUSSION

Synthesis and Characterization of Benzimidazolo-Chlorin Derivatives. In this study, we modified Pandey et al.'s[24] and our lab's[26] previous synthetic methods. Benzimidazolo-chlorins were synthesized from MPa **1** followed by a deacetylation and reduction reaction at the 13^2 position, as shown in Scheme 1. In the mixture of the three products, **3a** was the major compound (20% yield), followed by **3b** (10% yield) and **3c** (only 2.5% yield); this method differs slightly from our previous work.[26,27]

The two isomers **3a** and **3b** displayed quite different UV−vis absorption ranges (such as 730 and 714 nm of λ_{max}, respectively) (Figure 1), which was the same as previously reported by Pandey et al. and our lab.[24,26,27] When compared to **3a** and **3b**, compound **3c** had a lower wavelength absorption of λ_{max} at 708 nm. As a result, **3a** exhibited a highly red-shifted λ_{max} of 62 nm compared to that of MPPa **2**. Particularly, Pandey et al. confirmed the two isomer structures of **3a** and **3b** using single-crystal X-ray structures.[24]

Benzimidazolo-chlorin **3a** was characterized by ^{1}H-NMR spectroscopy (Figure S1), in which four new proton signals on the benzimidazole unit at 7.5−9.0 ppm in $CDCl_3$ appeared, indicating the successful formation of the benzimidazole ring in **3a**. The ^{13}C-NMR spectrum displayed all 40 carbon signals, demonstrating the distinct structure of **3a** (Figure S2). Furthermore, high-resolution fast atom bombardment mass spectrometry (HRFAB MS) analysis confirmed the formation

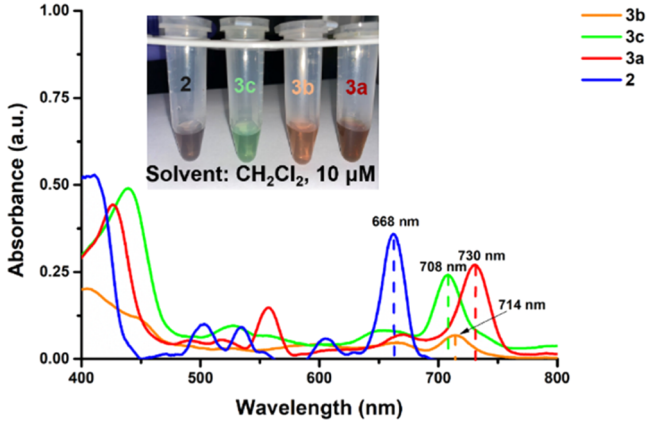

Figure 1. UV−vis absorption spectra of **2** and **3a**−**3c**. The concentration of the compound in each sample is 10 μM (CH_2Cl_2, 25 °C).

of **3a** (calcd for $[M + H]^+$ 651.3084; found 651.3086) (Figure S3). The fluorescence emission spectra (excitation wavelength, 730 nm) of **2** and **3a** revealed considerable fluorescence activity of the chlorins, with **3a** exhibiting a higher red-shift in the NIR region (745 nm) than **2** (675 nm, Figure 2). The significantly red-shifted UV−vis absorption and fluorescence

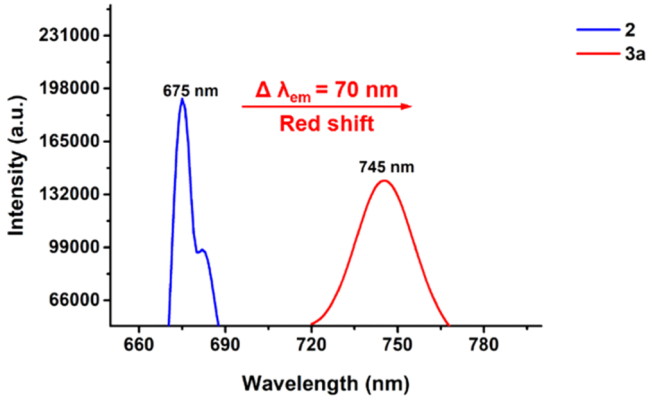

Figure 2. Fluorescence emission spectra of **2** and **3a**. The concentration of the compound in each sample is 20 μM (DMSO, 25 °C).

https://doi.org/10.1021/acsomega.3c01807
ACS Omega 2023, 8, 21941−21947

emission observed between **2** and **3a** could be attributed to the rigid conjugation of the benzene ring and imidazole ring, resulting in extended electron delocalization (Figure 3).

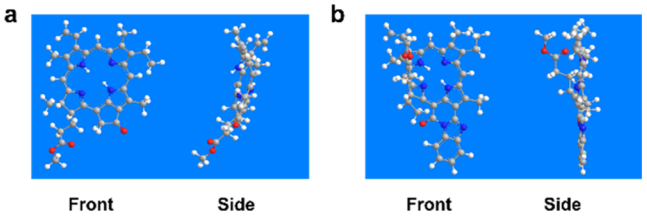

Figure 3. Energy-minimized ball-and-stick models of (a) **2** and (b) **3a**.

$^1O_2$ Photogeneration Study Using 1,3-Diphenylisobenzofuran (DPBF). The relative photodynamic effect of chlorin derivatives was evaluated through $^1O_2$ photogeneration ability using DPBF as a selective $^1O_2$ acceptor in the absence of tumor cells. In this study, we used two different LED lights (590−710 and 735−785 nm) to exhibit different activity effects depending on the absorption wavelength ranges of chlorins. The longer-wavelength LED having a 735−785 nm range is suitable for benzimidazolo-chlorin **3a** (λ_{max} of 730 nm) for generating enhanced $^1O_2$ photogeneration (Figures 4 and S4). In irradiation using a shorter-wavelength LED (590−710 nm), **3a** displayed better $^1O_2$ photogeneration compared with **2** and methylene blue (MB), which is a standard $^1O_2$ sensitizer. When irradiated with a longer-wavelength LED (735−785 nm), **3a** demonstrated more $^1O_2$ photogeneration than when exposed to a shorter-wavelength LED, while **2** and MB showed almost no $^1O_2$ photogeneration. Additionally, **3b** and **3c** exhibited comparable $^1O_2$ photogeneration using a shorter-wavelength LED (Figure S5). This indicates an absorption wavelength-dependent $^1O_2$ photogeneration for each PS molecule. We, therefore, selected **3a** as a suitable PS for further cell study in PDT based on its highest absorption wavelength of λ_{max} as well as $^1O_2$ photogeneration.

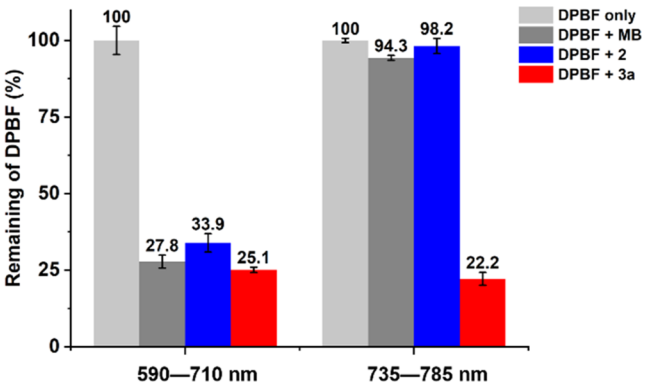

Figure 4. Remaining of DPBF (%, in DMSO) at 418 nm after photoirradiation using two LEDs (590−710 and 735−785 nm, total light dose of each LED: 2 J/cm^2; irradiation time: 15 min) without PSs (DPBF only, 50 μM) or the presence of PSs (1 μM) (without cells).

Cellular Uptake and Localization in Mitochondria and Lysosome. The successful cellular uptake and localization of **3a** in A549 and HeLa cells were confirmed by fluorescence images of **3a** using confocal laser scanning microscopy (CLSM, Figure 5).[28] CLSM images exhibited

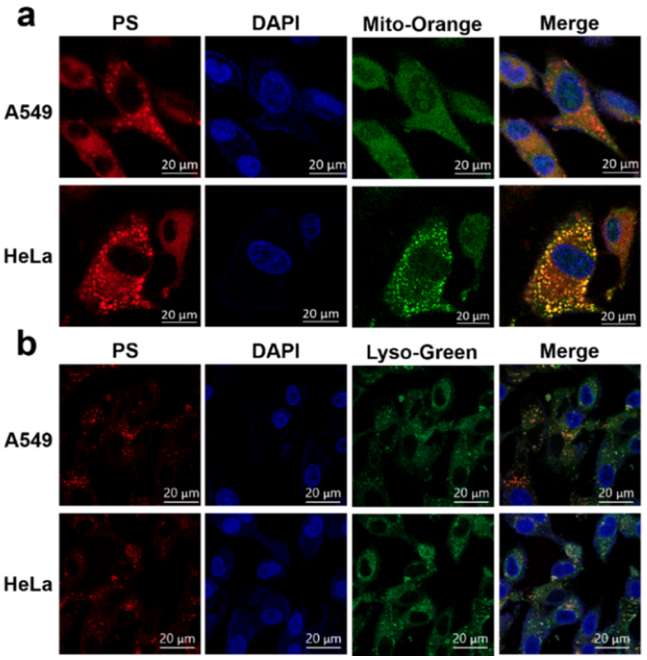

Figure 5. (a) Confocal images of **3a** (red) and mitochondria (green) in A549 and HeLa cells. (b) Confocal images of **3a** (red) and lysosome (green) in A549 and HeLa cells. Cells were treated with **3a** (5 μM) for 24 h post incubation by imaging with CLSM. Scale bar: 20 μm.

that **3a** displayed high mitochondria-targeted accumulation (Figure 5a), resulting in orange color in merged images and inducing mitochondria-mediated apoptosis to destroy the cancer cells.[29] And **3a** has low lysosome accumulation (Figure 5b), resulting in weak yellow color in merged images.

We conducted further quantitative evaluation of different organelle accumulations of **3a** for the signal colocalization using Pearson's correlation coefficient (PCC)[30] (Figure 6). For the mitochondria, PCC values were higher (0.520 and 0.733 in A549 and HeLa cells, respectively) than those in lysosome (0.265 and 0.267 in A549 and HeLa cells, respectively), indicating high mitochondria targeting (about 2−3 times) and low accumulation in lysosomes.

Cell Viabilities for Photocytotoxicity and Dark Cytotoxicity. The photocytotoxicity and dark toxicity of **2** and **3a** were evaluated in A549 and HeLa cells via the WST-8 assay at a range of 0.50−5.0 μM (Figure 7 and Tables S2−S5). Compounds **2** and **3a** demonstrated negligible dark toxicity, indicating their suitable biocompatibility. Upon irradiation with the longer-wavelength LED (735−785 nm, total light dose 2 J/cm^2), **3a** showed excellent photoactivity with half-maximum inhibitory concentration (IC_{50}, black dashed line in Figure 7) of 4.0 and 3.4 μM against A549 and HeLa cells, respectively. However, **2** exhibited negligible photoactivity. These results are consistent with $^1O_2$ photogeneration shown in Figure 4.

CONCLUSIONS

To develop a long-wavelength (NIR) absorbing PS, we revisited the synthesis of benzimidazolo-chlorin isomers **3a** and **3b** and fused them with quinoxaline **3c** derived through a one-step reaction between MPPa **2** and 1,2-phenylenediamine. Among the mixture of three products, **3a** has several advantages, including the following: (i) the major compound

https://doi.org/10.1021/acsomega.3c01807
ACS Omega 2023, 8, 21941−21947

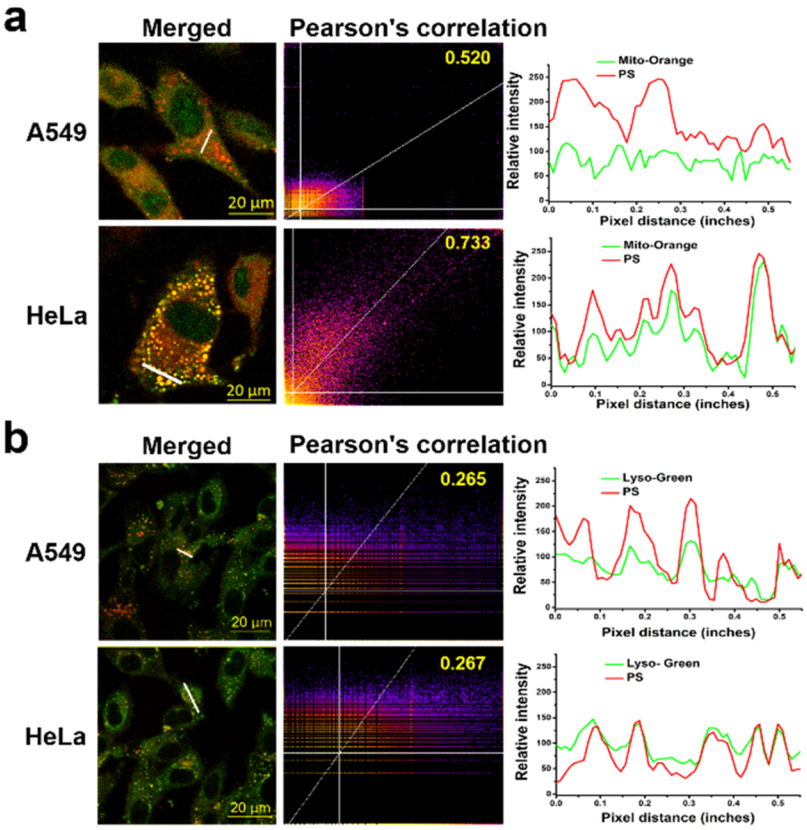

Figure 6. (a) Colocalization of **3a** (red) and mitochondria (green) in A549 and HeLa cells. (b) Colocalization of **3a** (red) and lysosome (green) in A549 and HeLa cells. PCC was calculated from the region of merged images (white line). The 2D intensity histogram and relative intensity are shown.

in the mixture; (ii) the longest absorption wavelength of λ_{max} at 730 nm; and (iii) the highest $^1O_2$ photogeneration. As a result, we evaluated **3a** in further cell studies. Long-wavelength absorbing benzimidazolo-chlorin **3a** displayed negligible dark toxicity and excellent phototoxicity, with an IC_{50} of 4.0 and 3.4 μM against A549 and HeLa cells, respectively, which might be attributed to cellular uptake followed by mitochondrial-targeting-mediated apoptosis for destroying tumor cells. This study will be useful in developing the design and synthesis of long-wavelength absorbing PS with high $^1O_2$ photogeneration and no dark toxicity, in addition to mitochondrial-targeting PS-mediated apoptosis for enhanced PDT.

EXPERIMENTAL SECTION

Materials. Chlorophyll-a paste was purchased from Shandong Lanmo Biotech Co., Ltd. (Shandong, China). Pyridine, dichloromethane, acetone, hydrochloric acid (35.0−37.0%), trifluoroacetic acid, urea, diethyl ether, and dimethyl sulfoxide were supplied by SAMCHUN (Pyeongtaek, Korea). Silica gel powder (SL−110−60 Å) was purchased from SK Chemicals Co., Ltd. (Gyeonggi-do, Korea). 1,2-Phenylenediamine, methylene blue (MB), and 1,3-diphenylisobenzofuran (DPBF) were purchased from Tokyo Chemical Industry, Ltd. (Tokyo, Japan). Methylamine hydrochloride was purchased from Sigma-Aldrich (St. Louis, MO). Sulfuric acid and potassium hydroxide were supplied from Duksan Pure Chemical Co. (Ansan-si, Korea). Dulbecco's modified Eagle's Medium, and Roswell Park Memorial Institute 1640 Medium were supplied from GenDPOT (Barker, TX). Fetal bovine serum (FBS) and streptomycin−penicillin were purchased from BioWest (Nuaillé, France). The cancer cell lines (A549 and HeLa) were purchased from the Korea Cell Line Bank (Seoul, Korea). WST-8 Cell Viability Assay Kit was supplied from Quanti-Max (Biomax, Gyeonggi-do, South Korea). 4′,6-Diamidino-2-phenylindole and MitoSpy Orange CMTMRos were supplied from BioLegend (San Diego, California). LysoTracker Green DND-26 was supplied from Invitrogen (Massachusetts). All compounds are 99−98% pure by HPLC analysis.

$^1O_2$ Photogeneration Study. DPBF was used to detect the formation of $^1O_2$. DPBF solution in DMSO (50 μM) was prepared in the dark using the following: DPBF only (50 μM, control sample) as a control group, MB (1 μM, containing DPBF), **2** (1 μM, containing DPBF), and **3a** (1 μM, containing DPBF). The samples were irradiated (2 J/cm^2) with LED for 15 min, after which the absorbance of each sample was measured at 418 nm using a fluorescence multidetection reader.

*Synthesis of MPPa (**2**).* MPa, **1** (5 g), was dissolved in 200 mL of pyridine and 5 mL of water, refluxed for 9 h under N_2, and then put into a diluted hydrochloric acid aqueous solution (1%). The solvent was evaporated under vacuum, and pure **2** (3.5 g) was obtained by recrystallization from dichloromethane and methanol. UV−vis (CH_2Cl_2) λ_{max} (log ε): 371.0 (4.44), 391.9 (4.44), 395.3 (4.44), 419.3 (4.44), 476.4 (3.61), 507.5 (4.00), 539.0 (3.91), 610.2 (3.86), 668.2 (4.37).

*Synthesis of Benzimidazolochlorophyll-a Methyl Ester (**3a**).* **2** (170 mg, 0.302 mmol) was dissolved in pyridine (15 mL), 1,2-phenylenediamine hydrochloride (65 mg) was added, and trifluoroacetic acid (0.5 mL) was injected into the

https://doi.org/10.1021/acsomega.3c01807
ACS Omega 2023, 8, 21941−21947

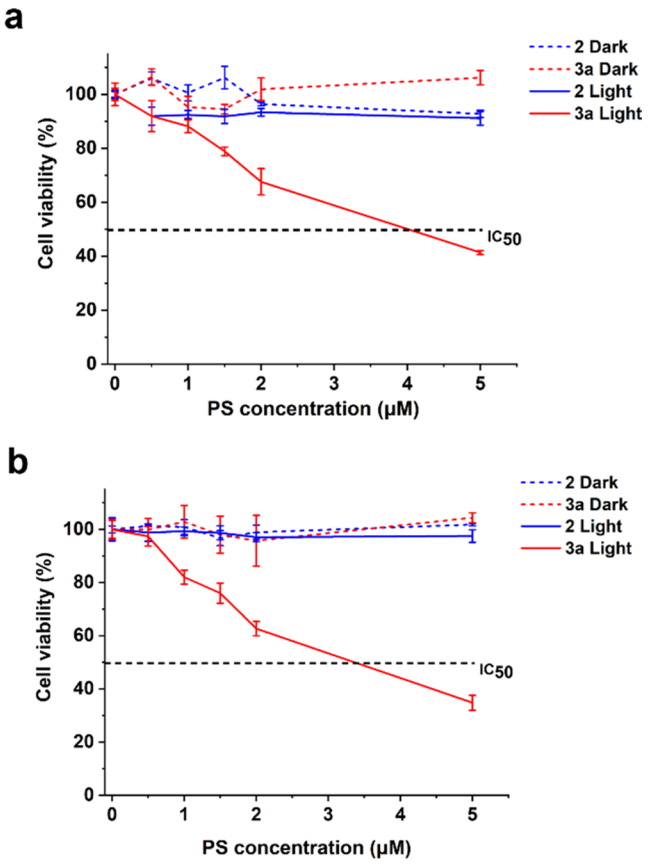

Figure 7. *In vitro* cell viability of **2** and **3a** in (a) A549 cells and (b) HeLa cells. Cell viability results in the dark (dash line) and irradiation of 735−785 nm (total light dose: 2 J/cm^2; irradiation time: 15 min) (solid line). PS concentration range: 0−5.0 μM.

solution. The reaction mixture was refluxed for 8 h, and the progress was monitored by thin-layer chromatography. The reaction solution was extracted using water and CH_2Cl_2 (500 mL). The organic layer was then dried over sodium sulfate, filtered, and removed under vacuum. The residue was treated with CH_2N_2 for 5 min and chromatographed on silica (eluent, toluene/acetone = 10:1), and the product was separated as a red-brown band (40 mg, yield 20%). UV−vis (CH_2Cl_2) λ_{max} (log ε): 377.8 (3.54), 427.2 (4.34), 487.3 (3.41), 516.0 (3.43), 557.2 (3.87), 668.8 (3.54) 730.7 (4.13). ^{1}H-NMR (500 MHz, $CDCl_3$) δ 9.33 (s, 1H, 10H), 9.22 (s, 1H, 5H), 8.95−8.87 (m, 1H, Ar-H^d), 8.75 (s, 1H, 20H), 8.05 (d, 1H, Ar-H^a), 7.99 (dd, J = 17.8, 11.5 Hz, 1H 3^{1}H), 7.65−7.56 (m, 2H, Ar-H^{b+c}), 6.51−6.18 (m, 2H, 3^{2}H), 5.62 (dd, J = 9.1, 2.6 Hz, 1H, 18H), 4.57 (q, J = 7.4 Hz, 1H, 17H), 3.80 (s, 3H, 12H), 3.54 (d, J = 10.3 Hz, 5H, 8^{1}H + 17^{3}H), 3.50 (s, 3H, 7^{1}H), 3.11 (s, 3H, 2^{1}H), 2.98 (dd, J = 15.4, 10.3, 4.7 Hz, 1H 17^1), 2.75−2.52 (m, 2H, 17^{1}H + 17^{2}H), 2.23 (tdd, J = 12.2, 8.8, 3.7 Hz, 1H, 17^{2}H), 2.02 (d, J = 7.4 Hz, 3H, 18^{1}H), 1.70 (t, J = 7.6 Hz, 3H, 8^{2}H), 1.59−1.37 (m, 1H, NH). HRFAB MS: calcd for $C_{37}H_{41}N_5O_4$ $[M + H]^+$ 651.3084; found, 651.3086.

Cellular Culture. HeLa (human cervical carcinoma) and A549 (human breast adenocarcinoma) cells were used in this study. The cells were cultured in DMEM and RPMI-1640 supplemented with 10% FBS and 1% antibiotics (streptomycin−penicillin) at 37 °C under a 5% humidified CO_2. The cells were collected by centrifugation, resuspended in the medium, and detected.

Cellular Uptake. To study the cellular uptake of PS, the cells were seeded in a confocal dish (2×10^4 cells) and incubated for 24 h. Subsequently, the cells were incubated for 24 h with free PS (5 μM). The cells were washed with PBS and stained with MitoTracker Orange and DAPI for 15 min. Images of the cells were acquired using a highly sensitive CLSM.

Cell Viability. A549 and HeLa cells were cultured in a suitable cell media at 37 °C in a 5% humidified CO_2 atmosphere. The cells were seeded into 48-well plates and incubated with different concentrations of **3a** for 24 h. After incubation, the cells were exposed to LED light irradiation for 15 min under 735−785 nm (for the dark toxicity experiment, LED light irradiation is not required), followed by an additional incubation of 24 h in the same conditions. The standard WST-8 assay (100 μL, 1:10 dilution of media) was used to measure cell viability for 1 h post incubation, and the results were expressed as a percentage of live cells relative to control cells.

■ ASSOCIATED CONTENT

Supporting Information

The Supporting Information is available free of charge at https://pubs.acs.org/doi/10.1021/acsomega.3c01807.

Experimental procedures, table of absorbance of PSs, images of DPBF experiments, ^{1}H-NMR and ^{13}C-NMR spectra, HRFAB mass spectrum of **3a**, and table of cell viability of PSs (PDF)

■ AUTHOR INFORMATION

Corresponding Authors

Jiazhu Li − *College of Chemistry and Chemical Engineering, Yantai University, Yantai, Shandong 264005, China*; Email: jiazhu82@ytu.edu.cn

Woo Kyoung Lee − *Center for Nano Manufacturing and Department of Nanoscience and Engineering, Inje University, Gimhae, Gyeongnam 50834, Republic of Korea*; Email: wlee@inje.ac.kr

Il Yoon − *Center for Nano Manufacturing and Department of Nanoscience and Engineering, Inje University, Gimhae, Gyeongnam 50834, Republic of Korea*; orcid.org/0000-0002-8562-1505; Email: yoonil71@inje.ac.kr

Authors

Huiqiang Wu − *Center for Nano Manufacturing and Department of Nanoscience and Engineering, Inje University, Gimhae, Gyeongnam 50834, Republic of Korea*

Sooho Yeo − *Center for Nano Manufacturing and Department of Nanoscience and Engineering, Inje University, Gimhae, Gyeongnam 50834, Republic of Korea*

Jinjun Wang − *College of Food & Biological Engineering, Yantai Institute of Technology, Yantai, Shandong 264005, China*

Complete contact information is available at: https://pubs.acs.org/10.1021/acsomega.3c01807

Author Contributions

Conceptualization was done by H.W., J.L., W.K.L., and I.Y.; methodology was done by H.W., S.Y., and J.W.; resource gathering was done by W.K.L. and I.Y.; writing and original draft preparation were done by H.W. and I.Y.; funding acquisition was done by W.K.L. and I.Y.; and supervision was

https://doi.org/10.1021/acsomega.3c01807
ACS Omega 2023, 8, 21941−21947

done by J.L., W.K.L., and I.Y. All authors have read and agreed to the published version of the manuscript.

Notes

The authors declare no competing financial interest.

■ ACKNOWLEDGMENTS

This research was supported by the National Research Foundation of Korea (NRF) grant, the Basic Science Research Program through the National Research Foundation of Korea (NRF) funded by the Ministry of Education (MOE, Korea, NRF-2020R1I1A1A01060632), and the Korean government (MSIT) (NRF-2020R1F1A1070571).

■ ABBREVIATIONS USED

PDT, photodynamic therapy; PS, photosensitizer; $^1O_2$, singlet oxygen; MPPa, methyl pyropheophorbide-a; NIR, near-infrared; MPa, methyl pheophorbide-a; DPBF, 1,3-diphenylisobenzofuran; MB, methylene blue; DMSO, dimethyl sulfoxide; CLSM, confocal laser scanning microscopy; PCC, Pearson's correlation coefficient; FBS, fetal bovine serum; PBS, phosphate-buffered saline; DMEM, Dulbecco's modified Eagle's medium; RPMI, Roswell Park Memorial Institute 1640 Medium; DAPI, 4′,6-diamidino-2-phenylindole

■ REFERENCES

(1) (a) Lucky, S. S.; Soo, K. C.; Zhang, Y. Nanoparticles in photodynamic therapy. *Chem. Rev.* **2015**, *115*, 1990−2042. (b) Yeo, S.; Song, H. H.; Kim, M. J.; Hong, S.; Yoon, I.; Lee, W. K. Synthesis and design of purpurin-18-loaded solid lipid nanoparticles for improved anticancer efficiency of phtodynamic therapy. *Pharmaceutics* **2022**, *14*, 1064. (c) Yeo, S.; Yoon, I.; Lee, W. K. Design and characterisation of pH-responsive photosensitiser-loaded nano-transfersomes for enhanced photodynamic therapy. *Pharmaceutics* **2022**, *14*, 210.

(2) Li, X.; Lee, S.; Yoon, J. Supramolecular photosensitizers rejuvenate photodynamic therapy. *Chem. Soc. Rev.* **2018**, *47*, 1174−1188.

(3) Feofanov, A.; Grichine, A.; Karmakova, T.; Pljutinskaya, A.; Lebedeva, V.; Filyasova, A.; Yakubovskaya, R.; Mironov, A.; Egret-Charlier, M.; Vigny, P. Near-infrared photosensitizer based on a cycloimide derivative of chlorin p6: 13,15-N-(3′-hydroxypropyl)-cycloimide chlorin p6. *Photochem. Photobiol.* **2002**, *75*, 633.

(4) Rkein, A. M.; Ozog, D. M. Photodynamic therapy. *Dermatol. Clin.* **2014**, *32*, 415−425.

(5) Kwiatkowski, S.; Knap, B.; Przystupski, D.; Saczko, J.; Kędzierska, E.; Knap-Czop, K.; Kotlińska, J.; Michel, O.; Kotowski, K.; Kulbacka, J. Photodynamic therapy−mechanisms, photosensitizers and combinations. *Biomed. Pharmacother.* **2018**, *106*, 1098−1107.

(6) Kharkwal, G. B.; Sharma, S. K.; Huang, Y.-Y.; Dai, T.; Hamblin, M. R. Photodynamic therapy for infections: clinical applications. *Lasers Surg. Med.* **2011**, *43*, 755−767.

(7) Sperandio, F.; Huang, Y.-Y.; Hamblin, M. R. Antimicrobial photodynamic therapy to kill gram-negative bacteria. *Recent Pat. Antiinfect. Drug Discovery* **2013**, *8*, 108−120.

(8) Celli, J. P.; Spring, B. Q.; Rizvi, I.; Evans, C. L.; Samkoe, K. S.; Verma, S.; Pogue, B. W.; Hasan, T. Imaging and photodynamic therapy: mechanisms, monitoring, and optimization. *Chem. Rev.* **2010**, *110*, 2795−2838.

(9) Lan, M.; Zhao, S.; Liu, W.; Lee, C. S.; Zhang, W.; Wang, P. Photosensitizers for photodynamic therapy. *Adv. Healthcare Mater.* **2019**, *8*, No. 1900132.

(10) Lin, H.; Lin, Z.; Zheng, K.; Wang, C.; Lin, L.; Chen, J.; Song, J. Near-infrared-II nanomaterials for fluorescence imaging and photodynamic therapy. *Adv. Opt. Mater.* **2021**, *9*, No. 2002177.

(11) Rybczynski, P.; Smolarkiewicz-Wyczachowski, A.; Piskorz, J.; Bocian, S.; Ziegler-Borowska, M.; Kędziera, D.; Kaczmarek-Kędziera, A. Photochemical properties and stability of BODIPY dyes. *Int. J. Mol. Sci.* **2021**, *22*, No. 6735.

(12) Chu, Y.; Xu, X.-Q.; Wang, Y. Ultra-Deep Photothermal therapy strategies. *J. Phys. Chem. Lett.* **2022**, *13*, 9564−9572.

(13) Huang, P.; Zhang, B.; Yuan, Q.; Zhang, X.; Leung, W.; Xu, C. Photodynamic treatment with purpurin 18 effectively inhibits triple negative breast cancer by inducing cell apoptosis. *Lasers Med. Sci.* **2021**, *36*, 339−347.

(14) Tracy, E. C.; Bowman, M. J.; Pandey, R. K.; Henderson, B. W.; Baumann, H. Cell-type selective phototoxicity achieved with chlorophyll-a derived photosensitizers in a co-culture system of primary human tumor and normal lung cells. *Photochem. Photobiol.* **2011**, *87*, 1405−1418.

(15) Zenkevich, E.; Sagun, E.; Knyukshto, V.; Shulga, A.; Mironov, A.; Efremova, O.; Bonnett, R.; Songca, S. P.; Kassem, M. Photophysical and photochemical properties of potential porphyrin and chlorin photosensitizers for PDT. *J. Photochem. Photobiol., B Biol.* **1996**, *33*, 171−180.

(16) Pandey, S. K.; Sajjad, M.; Chen, Y.; Pandey, A.; Missert, J. R.; Batt, C.; Yao, R.; Nabi, H. A.; Oseroff, A. R.; Pandey, R. K. Compared to purpurinimides, the pyropheophorbide containing an iodobenzyl group showed enhanced PDT efficacy and tumor imaging (^{124}I-PET) ability. *Bioconjugate Chem.* **2009**, *20*, 274−282.

(17) Hoober, J. K.; Sery, T. W.; Yamamoto, N. Photodynamic sensitizers from chlorophyll: purpurin-18 and chlorin p6. *Photochem. Photobiol.* **1988**, *48*, 579−582.

(18) Björn, L. O.; Papageorgiou, G. C.; Blankenship, R. E.; Govindjee. A viewpoint: why chlorophyll a? *Photosynth. Res.* **2009**, *99*, 85−98.

(19) Janssens, F.; Torremans, J.; Janssen, M.; Stokbroekx, R. A.; Luyckx, M.; Janssen, P. A. J. New antihistaminic N-heterocyclic 4-piperidinamines. 1. synthesis and antihistaminic activity of N-(4-piperidinyl)-1H-benzimidazol-2-amines. *J. Med. Chem.* **1985**, *28*, 1925−1933.

(20) Bansal, Y.; Minhas, R.; Singhal, A.; Arora, R. K.; Bansal, G. Benzimidazole: a multifacted nucelus for anticancer agents. *Curr. Org. Chem.* **2021**, *25*, 669−694.

(21) Bansal, Y.; Silakari, O. The therapeutic journey of benzimidazoles: a review. *Bioorg. Med. Chem.* **2012**, *20*, 6208−6236.

(22) Suraru, S. L.; Würthner, F. Strategies for the synthesis of functional naphthalene diimides. *Angew. Chem., Int. Ed.* **2014**, *53*, 7428−7448.

(23) Li, C.; Zhu, L.; Liang, W.; Su, R.; Yin, J.; Hu, Y.; Lan, Y.; Wu, D.; You, J. An unusual [4 + 2] fusion strategy to forge: meso-N/O-heteroarene-fused (quinoidal) porphyrins with intense near-infrared Q-bands. *Chem. Sci.* **2019**, *10*, 7274−7280.

(24) Kozyrev, A. N.; Suresh, V.; Das, S.; Senge, M. O.; Shibata, M.; Dougherty, T. J.; Pandey, R. K. Syntheses and spectroscopic studies of novel chlorins with fused quinoxaline or benzimidazole ring systems and the related dimers with extended conjugation. *Tetrahedron* **2000**, *56*, 3353−3364.

(25) Kozyrev, A.; Ethirajan, M.; Chen, P.; Ohkubo, K.; Robinson, B. C.; Barkigia, K. M.; Fukuzumi, S.; Kadish, K. M.; Pandey, R. K. Synthesis, photophysical and electrochemistry of near-IR absorbing bacteriochlorins related to bacteriochlorophyll a. *J. Org. Chem.* **2012**, *77*, 10260−10271.

(26) Zhang, Z.; Zhao, Y.; Wang, X.; Li, J.; Wang, J. Syntheses of chlorophyllous chlorin derivatives with aromatic ring-fused imidazole structural unit. *Chin. J. Org. Chem.* **2021**, *41*, 1177−1186.

(27) Liu, R.; Wang, L.; Yin, J.; Wu, J.; Liu, C.; Zhang, P.; Wang, J. Synthesis of benzimidazolo-fused purpurin-18 derivatives with the basic skeleton of chlorophyll. *Chin. J. Org. Chem.* **2012**, *32*, 318−325.

(28) Liu, Y.; Lee, S. H.; Lee, W. K.; Yoon, I. Ionic liquid-dependent gold nanoparticles of purpurin-18 for cellular imaging and photodynamic therapy in vitro. *Bull. Korean Chem. Soc.* **2020**, *41*, 230−233.

(29) (a) Lee, T. H.; Liu, Y.; Kim, H. J.; Lee, S. H.; Song, H. H.; Shim, Y. K.; Lee, W. K.; Yoon, I. Mitochondrial targeting cationic purpurinimide−polyoxometalate supromolecular complexes for enhanced photodynamic therapy with reduced dark toxicity. *Eur. J.*

https://doi.org/10.1021/acsomega.3c01807
ACS Omega 2023, 8, 21941−21947

Inorg. Chem. **2021**, 3211−3223. (b) Liu, Y.; Lee, T. H.; Lee, S. H.; Li, J.; Lee, W. K.; Yoon, I. Mitochondria-targeted water-soluble organic nanoparticles of chlorin derivatives for biocompatible photodynamic therapy. *ChemNanoMat* **2020**, *6*, 610−617.
(30) Byun, G.; Kim, S.-Y.; Choi, M.-W.; Yang, J.-K.; Kwon, J. E.; Kim, S.; Park, S. Y. Highly photostable fluorescent proves for multi-color and super-resolution imaging of cell organelles. *Dyes Pigm.* **2022**, *204*, No. 110427.

https://doi.org/10.1021/acsomega.3c01807
ACS Omega 2023, 8, 21941−21947